Molecular Therapy
Methods & Clinical Development
Original Article

# Evaluation of two *in vitro* assays for tumorigenicity assessment of CRISPR-Cas9 genome-edited cells

Myriam Lemmens,[1,2] Benoit Fischer,[1] Michael Zogg,[1,4] Lindsey Rodrigues,[1,5] Grainne Kerr,[1] Alberto del Rio-Espinola,[1] Fanny Schaeffer,[1] Danilo Maddalo,[1,6] Valerie Dubost,[1] Alessandro Piaia,[1] Arne Mueller,[1] Ulla Plappert-Helbig,[1,7] Ulrike Naumann,[1] Jasmin Haegele,[1] Alex Odermatt,[3] Hans-Jörg Martus,[1] and Silvana Libertini[1]

[1]Novartis Institutes for BioMedical Research, 4057 Basel, Switzerland; [2]University of Basel, 4001 Basel, Switzerland; [3]Department of Pharmaceutical Sciences, University of Basel, 4056 Basel, Switzerland

**Off-target editing is one of the main safety concerns for the use of CRISPR-Cas9 genome editing in gene therapy. These unwanted modifications could lead to malignant transformation, which renders tumorigenicity assessment of gene therapy products indispensable. In this study, we established two *in vitro* transformation assays, the soft agar colony-forming assay (SACF) and the growth in low attachment assay (GILA) as alternative methods for tumorigenicity evaluation of genome-edited cells. Using a CRISPR-Cas9-based approach to transform immortalized MCF10A cells, we identified *PTPN12*, a known tumor suppressor, as a valid positive control in GILA and SACF. Next, we measured the limit of detection for both assays and proved that SACF is more sensitive than GILA (0.8% versus 3.1% transformed cells). We further validated SACF and GILA by identifying a set of positive and negative controls and by testing the suitability of another cell line (THLE-2). Moreover, in contrast to SACF and GILA, an *in vivo* tumorigenicity study failed to detect the known tumorigenic potential of PTPN12 deletion, demonstrating the relevance of GILA and SACF in tumorigenicity testing. In conclusion, SACF and GILA are both attractive and valuable additions to preclinical safety assessment of gene therapy products.**

## INTRODUCTION

In 2021, more than a dozen clinical trials involving CRISPR-Cas9 genome editing have been listed on the ClinicalTrials.gov database. With the use of the CRISPR-Cas9 technology in gene therapy burgeoning, its long-term safety for patients is of concern. To date, safety implications are uncertain and a lack of a global consensus on preclinical safety assessment of genome-edited products calls for clear strategies. Safety concerns are, among others, Cas9-mediated cleavage in undesired DNA regions (off-target editing),[1–3] genomic rearrangements,[4,5] including chromothripsis[6] or other large-scale chromosomal aberrations[7] that potentially lead to genomic instability, and malignant transformation of genome-edited cells in patients.[8,9] For this reason, evaluating the tumorigenicity of a gene therapy product is of paramount relevance for the safety of these approaches. The World Health Organization defines tumorigenicity as "the capacity of a cell population inoculated into an animal model to produce a tumor by proliferation at the site of inoculation and/or at a distant site by metastasis."[10] Currently, *in vivo* tumorigenicity studies, in which human cells are injected ectopically into immune-suppressed mice and monitored for tumor formation, are considered conventional assays for tumorigenicity assessment.[10–14] However, the engraftment rate of human tumor tissue in non-obese diabetic (NOD) severe combined immunodeficiency (SCID) γ (NSG) mice is highly variable and, based on the tissue type and aggressiveness of the tumor, can range from 25% to 80%,[15–19] which questions the predictability of human tumor formation in immune-compromised mice. Moreover, following implantation, *in vivo* tumor formation should be observed for at least 6 months and,[20] for some cell types, up to 12 months,[21,22] which makes such experiments time- and resource-consuming. As a consequence, alternative *in vitro* transformation assays have been proposed for safety assessment.[11,23] These assays monitor one or several phenotypic alterations caused by cancerous transformation, such as anchorage-independent growth, disorganized patterns of colony growth, or alterations of cell morphology after treatment with chemicals or other manipulations.[24] Given the challenges of *in vivo* studies, the use of *in vitro* assays could provide valuable safety information and potentially accelerate safety testing for cell and gene therapy products. Additionally, *in vitro* assays offer animal welfare

Received 26 March 2021; accepted 3 September 2021;
https://doi.org/10.1016/j.omtm.2021.09.004.

[4]Present address: Department of Pharmaceutical Sciences, University of Basel, 4056 Basel, Switzerland

[5]Present address: Epizyme, Cambridge, MA 02139, USA

[6]Present address: Department of Translational Oncology, Genentech, Inc., South San Francisco, CA 94080, USA

[7]Present address: 79539 Lörrach, Germany

**Correspondence:** Silvana Libertini, PhD, Novartis Institutes for BioMedical Research, Klybeckstrasse 141, 4057 Basel, Switzerland.
**E-mail:** silvana.libertini@novartis.com


This is an open access article under the CC BY-NC-ND license (http://creativecommons.org/licenses/by-nc-nd/4.0/).

benefits and align with the 3Rs (replacement, refinement, and reduction) principle of animal use.[25]

The soft agar colony-forming assay (SACF) is an *in vitro* transformation assay based on anchorage-independent growth. Hamburger and Salmon[26] and Salmon et al.[27] demonstrated that, in contrast to adherent non-tumorigenic cells, tumorigenic cells are able to grow anchorage independently in soft agar and used this feature to develop SACF to evaluate the chemosensitivity of human cancer cells to antitumoral treatments. Since then, SACF has been widely used to screen for effective chemotherapeutics[28–30] and to characterize whether non-tumorigenic cells acquired tumorigenic features,[31–33] among others, upon CRISPR-Cas9 mediated gene knockout.[34] Recently, Kusakawa et al.[23] published a miniaturized digital SACF for the detection of tumorigenic impurities of cell therapy products. The term "digital" arises from partitioning each sample into multiple wells, which enables the attribution of a digital output to each well ("positive" or "negative"). In comparison to a previously performed *in vivo* tumorigenicity study in NOD/Shi-SCID IL2Rγ null mice,[35] digital SACF was described as more sensitive and time-saving.[23] These studies suggested that SACF could be a useful assay for regulatory tumorigenicity testing of cell therapy products. An alternative *in vitro* transformation method to detect anchorage independency is the growth in low attachment assay (GILA). GILA is reported to correlate with SACF regarding the ability to assess cellular transformation,[36] and it has been used, for example, to monitor anchorage independency upon gene knockdown,[37] drug or substance treatment,[38,39] and for phenotypic screens.[36,40] In contrast to the colony count readout of SACF, growth of cells cultivated in low attachment plates is measured by quantifying ATP levels.

In the present study, we tested whether SACF and GILA could be used to detect the *in vitro* transformation potential of CRISPR-Cas9 genome-edited cells by knocking out tumor suppressors in MCF10A cells, an immortalized (non-transformed) mammary epithelial cell line, and we determined the limit of detection (LOD) of both assays. We also challenged these approaches on THLE-2 cells, an immortalized human cell line of hepatic origin. Finally, we compared the performance of both assays on MCF10A cells with an *in vivo* tumorigenicity study, showing that SACF and GILA could provide valuable safety information and have the potential for being included in a novel preclinical testing strategy for *ex vivo* genome-edited products.

## RESULTS

### Identification of the *PTPN12* gene as a positive control for *in vitro* transformation

For the validation of SACF and GILA as transformation assays for genome-edited cells, we focused on knockout editing, since precise knock in of defined DNA sequences is still a challenge.[41,42] As a consequence, the most advanced CRISPR-Cas9 gene therapies are based on the introduction of frameshift deletions or insertions, resulting in loss-of-function mutations in genes.[43] In this framework, a suitable positive control would be a guide RNA targeting a gene whose deletion leads to transformation, e.g., a tumor suppressor. In order to identify the most appropriate positive controls, we conducted a genome-wide CRISPR-Cas9 knockout screen based on the induction of proliferation as a readout.[44–46] Aberrant proliferation is a prominent feature of transformed cells, and thus genes involved in transformation could be identified among those responsible for hyperproliferation.[47] As a cellular model we used MCF10A cells, which are a spontaneously immortalized human mammary epithelial cell line.[48] Given that MCF10A cells are untransformed, acquired tumorigenic features such as anchorage independency and *in vivo* tumor growth can be monitored. We chose a human cell line since both on-target and off-target CRISPR-Cas9-mediated cleavages are sequence specific (hence species specific). The screen was performed by transducing MCF10A cells stably expressing Cas9 (MCF10A Cas9) with a lentiviral library of guide RNAs targeting all protein coding genes (approximately 20,000). Two weeks after infection, DNA was extracted and analyzed by next-generation sequencing (NGS) in order to determine overrepresented clones. As MCF10A cell growth is dependent on epidermal growth factor (EGF),[48] potential EGF independency could be associated with enhanced proliferation. Therefore, we conducted the screen in EGF-free and EGF-containing medium and selected the highest hits among both conditions.

The CRISPR-Cas9 screen revealed known tumor suppressor genes such as tumor protein p53 (*TP53*), phosphatase and tensin homolog (*PTEN*), neurofibromin 2 (*NF2*), ERBB receptor feedback inhibitor 1 (*ERRFI1*), cyclin-dependent kinase inhibitor 1A (*CDKN1A*), and tyrosine-protein phosphatase non-receptor type 12 (*PTPN12*) as the strongest inducers of hyperproliferation in MCF10A cells (Figure 1A). We first interrogated *PTPN12* as a positive control in SACF and GILA, since the induction of anchorage-independent growth upon PTPN12 deletion was previously reported in another human mammary epithelial cell (HMEC) line.[49] We ranked the CRISPR RNA (crRNA) sequences against *PTPN12* from the previously used crRNA library according to their ability to induce hyperproliferation and their *in silico* off-target profile determined by Cas-OFFinder software.[50] The three best performing crRNAs based on these two criteria were chosen for further evaluation. We electroporated MCF10A Cas9 cells with the CRISPR:tracr RNA (cr:trRNA) complexes and verified efficient PTPN12 knockout by estimating cleavage efficiency using Sanger sequencing followed by TIDE (tracking of indels by decomposition) analysis,[51] as well as protein depletion using western blotting (Figure 1B). Next, we determined whether PTPN12 deletion enabled anchorage-independent growth by testing MCF10A Cas9 cells in GILA and SACF plates immediately after electroporation with the respective cr:trRNA complex. To perform SACF (Figure 1C), cells were seeded in soft agar as a single-cell suspension and incubated for 4 weeks, which is sufficient time to allow transformed cells to form colonies, while non-transformed cells do not survive. Colonies were stained and features including size, shape, average intensity, and variation of the staining signal were measured to count colonies. Cells in GILA were incubated for 2 weeks before measuring ATP levels (Figure 1C). Results showed that deleting PTPN12 using any of the three chosen *PTPN12* crRNAs significantly led to increased

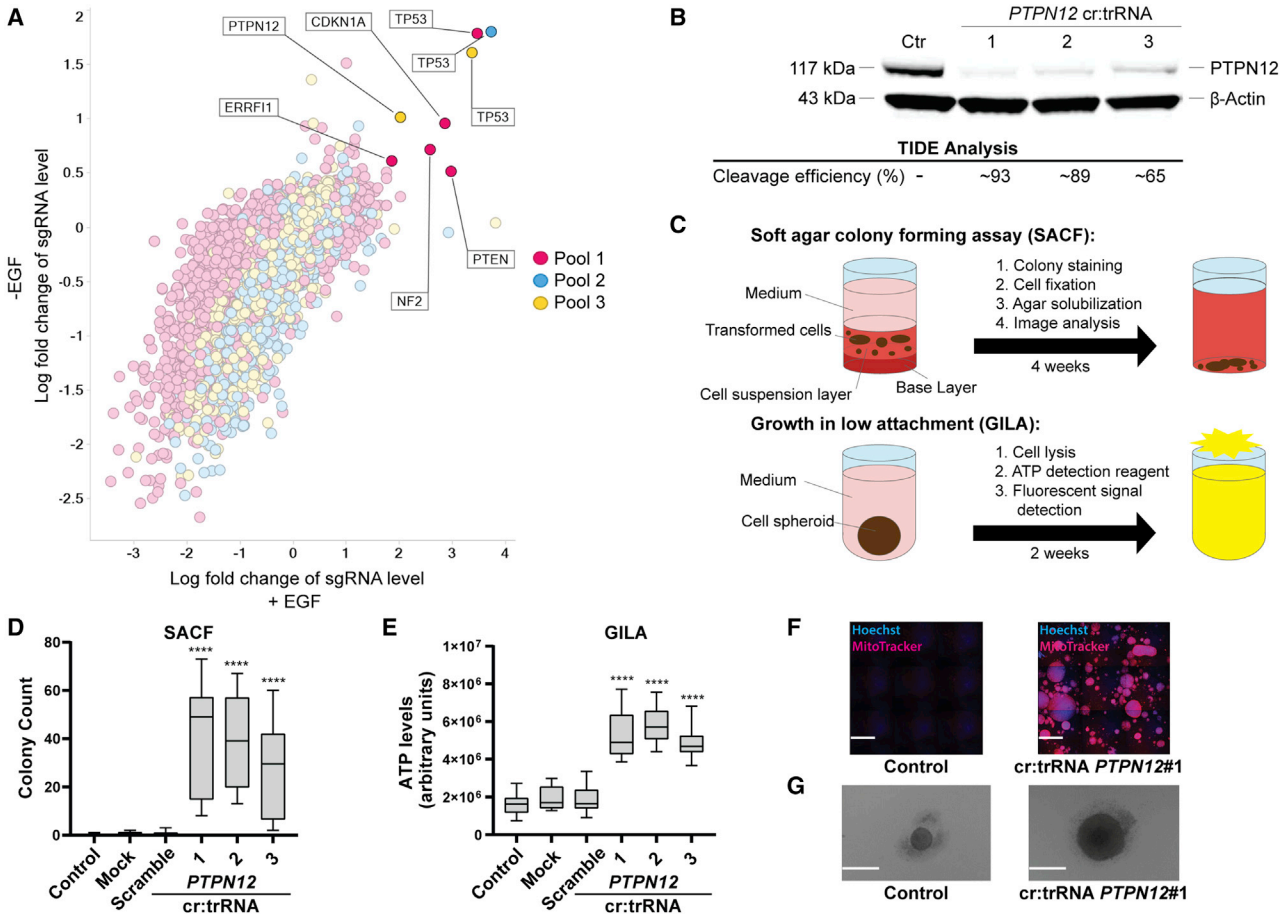


**Figure 1. Identification and validation of PTPN12 as positive control for SACF and GILA**

(A) To find genes whose deletion induces hyperproliferation, a genome-wide CRISPR-Cas9 knockout screen was performed. MCF10A Cas9 cells were transduced with three pools of a lentiviral library containing 66,000 sgRNAs each (10 sgRNAs/gene) against approximately 20,000 genes. After 2 weeks, DNA was extracted and analyzed by NGS. The screen was performed in the presence and absence of EGF. $Log_2$ fold change against internal controls of sgRNA levels was calculated to identify inducers of hyper-proliferation. (B) Three cr:trRNAs against *PTPN12* were electroporated into MCF10A Cas9 cells. 24 h after electroporation, cleavage efficiency was determined by TIDE analysis (lower part). Western blot analysis on protein lysates collected 1 week after electroporation confirmed PTPN12 knockout (upper part). (C) Schematic representation of SACF and GILA. For SACF, 2,500 cells/well were seeded in soft agar. Following 4 weeks of incubation, colonies were stained with Hoechst 33342 (to identify nuclei) and MitoTracker Red CMXRos (for live mitochondria), fixed, agar was solubilized and colonies were counted by a high-content imager. Solubilization was required to allow the colonies to sink to the bottom of the well in one plane, which enabled microscopic analysis. For GILA, 2,500 cells/well were seeded in low-attachment plates and incubated for 2 weeks before ATP level detection. (D and E) 150,000 MCF10A Cas9 cells were electroporated with three different cr:trRNA against *PTPN12*, and 2,500 cells/well, six wells/condition, were seeded in SACF (D) and GILA (E), respectively. As control samples, we used untreated cells ("Control"), cells electroporated without cr:trRNA ("Mock"), and cells electroporated with a non-targeting scramble cr:trRNA complex ("Scramble"). The data of three independent experiments are shown as boxplots. The boxes describe the inter-quartile range, the whiskers indicate the range from the minimum to the maximum values, and the line is equal to the median. Statistical analysis was performed on three assay repetitions using mixed linear regression models for negative binominal (SACF) or Gaussian distribution (GILA) with a post hoc Holm-Bonferroni p values adjustment. ****$p < 0.001$ (Data S1 and S2). The differences between the three independent experiments are represented in Figure S1. (F) Images of control and edited MCF10A Cas9 cells using cr:trRNA *PTPN12*#1 after 4 weeks in soft agar (montage of nine images, each taken with a 5× objective, wide field mode; scale bars, 1 mm). (G) Spheroids of control and edited MCF10A Cas9 cells grown in low-attachment plates for 2 weeks (images were take with a 4× objective, wide field mode; scale bars, 0.5 mm).

colony formation and growth in low attachment, with *PTPN12* cr:trRNA#1 being the most effective (Figures 1D–1G and S1). To further characterize the effect of PTPN12 deletion, we monitored the growth factor dependency of *PTPN12*-edited MCF10A Cas9 cells in restrictive culturing conditions. We concluded that PTPN12-deficient cells are less EGF-dependent than is their parental cell line (Figure S2).

### Detection limit of *in vitro* transformation assays using CRISPR-Cas9-edited cells

The LOD of SACF and GILA was determined using the best cr:trRNA cutter, *PTPN12*#1 (Figures 1D, 1E, and S1). We electroporated different amounts of cr:trRNA *PTPN12*#1, ranging from 0.5 to 12 pmol. Directly after electroporation, the cell suspension was divided into three aliquots to perform, from the same cell pool, SACF,

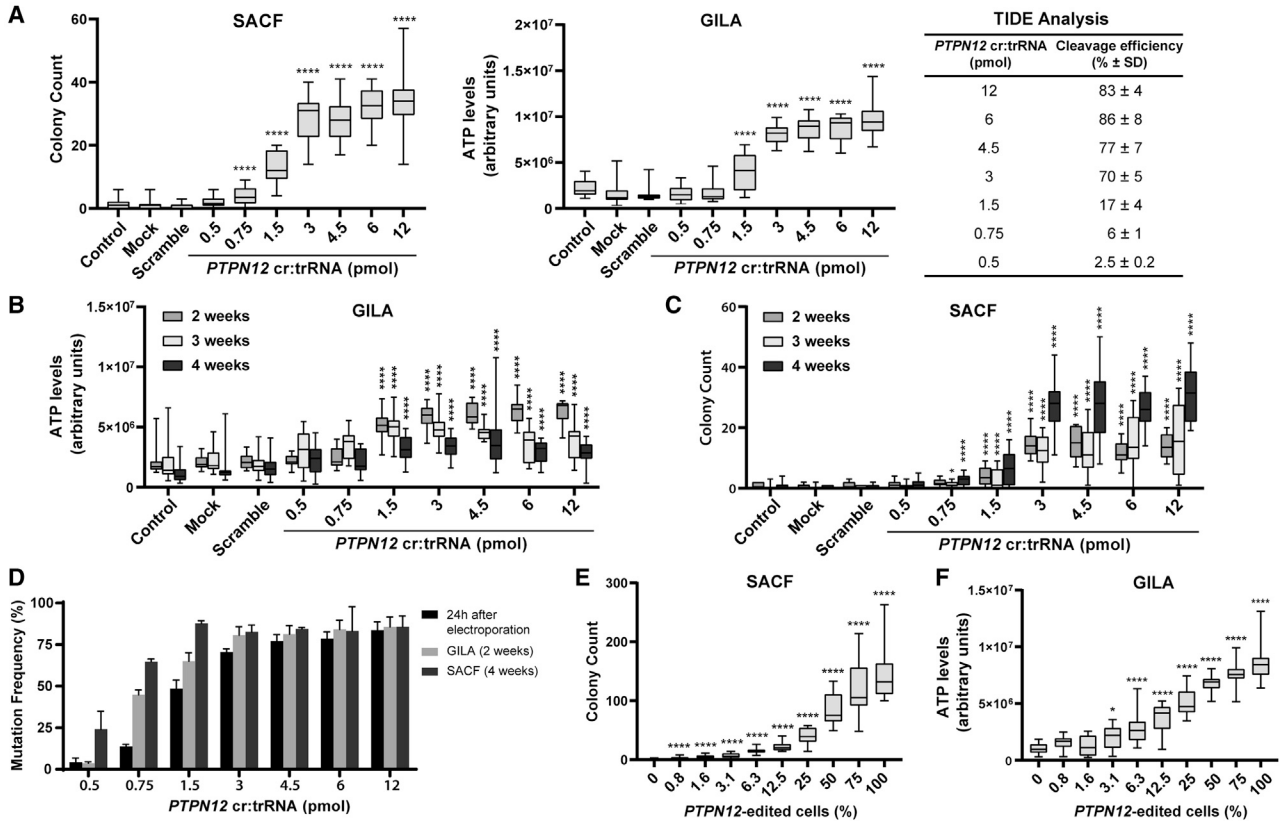


**Figure 2. LOD of SACF and GILA**

(A) The limit of detection (LOD) of SACF and GILA was determined by titrating the amount of cr:trRNA. 150,000 MCF10A Cas9 cells were electroporated with 0.5–12 pmol *PTPN12* cr:trRNA, and 2,500 cells/well, six wells per condition, were seeded for GILA and SACF, respectively. The remaining cells were used for cleavage efficiency analysis 24 h after seeding using Sanger sequencing data and TIDE tool. The table shows the cleavage efficiencies from three independent experiments as mean ± standard deviation (SD). (B and C) Cells electroporated with the indicated amount of crRNA:trRNA were seeded in low-attachment plates (GILA; B) or soft agar (SACF, C) and incubated for 2, 3, or 4 weeks to compare and determine the ideal incubation time. (D) Mutation frequencies of cells electroporated with different amounts of *PTPN12* cr:trRNA were obtained 24 h after electroporation, after a 2-week incubation in GILA and a 4-week incubation in SACF by using Sanger sequencing data and the TIDE analysis tool. DNA was sequenced in three technical replicates, which are represented in the graph as mean ± SD. (E and F) A pool of stably edited cells for the *PTPN12* gene was generated by electroporating MCF10A Cas9 cells with cr:trRNA *PTPN12*#1 and expanding for 4 weeks before conducting SACF and GILA. The LODs of SACF and GILA were determined by spiking the stable *PTPN12*-edited cells with parental MCF10A Cas9 cells. 2,500 cells/well were seeded for both SACF and GILA. All p values were calculated using the combined data of three assay repetitions using mixed linear regression models assuming negative binominal distribution for colony count and Gaussian distribution for ATP levels with post hoc Holm-Bonferroni p value adjustment (*$p < 0.05$, ****$p < 0.001$; see Data S1 and S2). Boxplots represent pooled data of three independent assay repetitions with six technical replicates each. See Figure S3 for a representation of the individual assay repetitions.

GILA, and cleavage efficiency analysis. Cleavage efficiency was evaluated 24 h after seeding, GILA after 2 weeks, and SACF after 4 weeks.

SACF showed a significant increase in colony count starting from a cr:trRNA amount of 0.75 pmol, which corresponds to 6% ± 1% of cleaved events, or ∼150 *PTPN12* mutated cells/well (Figures 2A and S3A). For GILA, the LOD corresponded to 1.5 pmol of the cr:trRNA complex (17% ± 4.3% cleavage efficiency determined by Sanger sequencing/TIDE analysis, or ∼425 mutated cells/well) (Figures 2A and S3B). To exclude that the poorer LOD in GILA was due to its shorter incubation time, we incubated GILA for 2, 3, or 4 weeks and found no improvement in the LOD at longer time points (Figures 2B and S3C). Next, we inquired whether SACF incubation time could be shortened to 2 or 3 weeks without affecting statistical significance levels. However, the highest statistically significant difference between edited and control groups was observed with an incubation time of 4 weeks (Figures 2C and S3D).

We hypothesized that the enhanced LOD seen in SACF was due to improved selection, since cells in SACF were cultivated as a single-cell suspension whereas cells seeded in low attachment plates form spheroids. Therefore, a mutated cell located inside a spheroid could receive stress signals by surrounding anchorage-dependent cells, which could prevent clonal expansion of the mutated cell. To test this hypothesis, we compared the amount of residual unedited cells 24 h after electroporation from colonies grown in SACF for 4 weeks

**Table 1. Cleavage efficiencies and sequences of crRNA for tested genes**

| Gene | crRNA sequence (5′ → 3′) | Cleavage efficiency (% ± SD) determined by TIDE |
|---|---|---|
| *PTEN* | ACCGCCAAAUUUAAUUGCAG | 85 ± 7 |
| *NF2* | CAGAGAGGUUUCAACACACC | 89 ± 3 |
| *ERRFI1* | CUAGAACCCCGUUCACAAAG | 83 ± 11 |
| *CDKN1A* | GAUGUCCGUCAGAACCCAUG | 72 ± 16 |
| *TP53#1* | GUAGUGGUAAUCUACUGGGA | 75 ± 7 |
| *TP53#2* | AAUCAACCCACAGCUGCACA | 25 ± 24 |
| *TP53#3* | UCCUCAGCAUCUUAUCCGAG | 41 ± 30 |
| *TP53#2+3* | AAUCAACCCACAGCUGCACA + UCCUCAGCAUCUUAUCCGAG | 27 ± 30 |
| *CYP26B1* | GUCCGGACACCGCCACCGAA | 84 ± 9 |
| *BDKRB2* | GCAGAAGGUGAUGACACUCA | 58 ± 16 |
| *CSN2#1* | UCAACGAAUGGAUAGAUCAG | 76 ± 14 |
| *CSN2#2* | ACAGGACUUAGUAGCCAUGA | 62 ± 5 |
| *Cas9*[52] | UACGCCGGCUACAUUGACGG | 59 ± 4 |
| *BCL11A*[6] | CUAACAGUUGCUUUUAUCAC | 24 ± 8 |

For each potential positive and negative control, the best cleaving crRNA was chosen for evaluation in SACF and GILA. The sequence of the selected crRNA and its respective cleavage efficiency determined by TIDE analysis are shown (three independent experiments, mean ± SD).

and from spheroids grown in GILA for 2 weeks. We confirmed that colonies in SACF consisted of a nearly homogeneous PTPN12-edited population up to a cr:trRNA dose of 0.75 pmol, while spheroids in GILA consisted of a mixed population of unedited and PTPN12-edited cells when less than 1.5 pmol *PTPN12* cr:trRNA was used (Figure 2D).

When assessing the transformation potential of *ex vivo* genome-engineered cells for gene therapy, cells are conventionally first edited and expanded before safety testing. Thus, besides testing the effect of *PTPN12* cr:trRNA directly after electroporation, we determined the LOD of stably edited MCF10A Cas9 cells that were generated using cr:trRNA *PTPN12*#1 and expanded for 4 weeks. After this time, we evaluated the mutation frequency by amplicon sequencing (∼87%) and verified protein depletion by western blot (Figure S4; Table S4). To estimate a LOD using this approach, we spiked the previously expanded *PTPN12*-edited cells in different ratios with parental MCF10A Cas9 cells and performed SACF as well as GILA. In this case, we were able to detect 0.8% ( =20 cells/well) edited cells in SACF and 3.1% (=79 cells/well) edited cells in GILA (Figure 2E, 2F, S3E, and S3F).

### Identification of further controls for CRISPR-Cas9-mediated *in vitro* transformation

Besides *PTPN12*, five other known tumor suppressors strongly induced hyperproliferation in the CRISPR-Cas9 screen: *TP53*, *PTEN*, *CDKN1A*, *ERFFI1*, and *NF2* (Figure 1A). Hence, we tested whether those genes could be positive controls for SACF and GILA. As previously described, we selected potential crRNAs for each gene based on their performance in the screen (Figure 1A) and evaluated their specificity according to Cas-OFFinder software.[50] Next, we assessed the cleavage efficiency of the selected crRNAs after 24 h, chose the best cleaving cr:trRNAs for each target (Table 1), and verified efficient protein knockout by western blot (Figure 3A). The electroporation with cr:trRNA *PTEN*, *CDKN1A*, *ERRFI1*, and *NF2* led to efficient protein depletion. The cr:trRNA *TP53*#1 did not result in protein depletion despite cleaving the DNA most efficiently. Therefore, further tr:crRNAs against *TP53* were tested, including two cr:trRNAs against *TP53* in combination. The cr:trRNAs *TP53*#2 and *TP53*#3 induced double-strand breaks in close proximity (100 bp) to each other and, when used in combination, lead to a removal of a DNA fragment (Figure S5) and TP53 protein loss (Figure 3A).

Additionally, in order to identify negative controls, we selected genes that neither influenced viability nor induced hyperproliferation in our screening: cytochrome p450 26B1 (*CYP26B1*), bradykinin receptor B2 (*BDKRB2*), casein beta (*CSN2*), and the bacterial *Cas9*. As for the tumor suppressor genes, we selected the best performing crRNA according to the CRISPR-Cas9 knockout screen, performed *in silico* off-target analysis, and selected the best cleaving crRNA for each gene by TIDE analysis (Table 1).

We then tested the ability of the selected genes to induce anchorage-independent growth in GILA and SACF (Figures 3B–3E and S6A–S6D) and we showed that ERRFI1, NF2, and PTEN deletion led to anchorage-independent growth in GILA as well as in SA*CF*. While NF2 deletion was a stronger positive control in SACF, PTEN deletion led to more statistically significant results in GILA. The neutral genes *CSN2*, *CYP26B1*, *BDKRB2*, and *Cas9* did not lead to anchorage independency in either assay. However, upon CSN2 deletion, we observed a slightly increased, but not statistically significant, colony count in one out of three SACF experiments that prompted us to further investigations. We performed SACF upon CSN2 deletion an additional three times and included another crRNA against *CSN2* (*CSN2*#2, Figure S7). Using this approach, we did not observe any colony growth and thus confirmed the negative result of CSN2 deletion. The deletion of the tumor suppressor genes *CDKN1A* and *TP53*, against which we tested several crRNA alone or in combination (*TP53*#2 and *TP53*#3), did not lead to significant increase of anchorage independency as well.

To determine the suitability of another cell line for *in vitro* transformation assays, we performed the same set of SACF and GILA experiments on THLE-2 cells (Figure S8), an immortalized human hepatic cell line.[53] In GILA, all of the positive controls identified in MCF10A Cas9 cells (*PTPN12*, *NF2*, *ERFFI1*, and *PTEN*) led to a significant increase in ATP levels in THLE-2 cells (Figures S8B and S8D). In contrast, the colony-forming efficiency of THLE-2 cells in SACF was substantially lower than for MCF10A cells (Figures S8C and S8E), leading to an accordingly lower and not significant difference in colony counts.

To demonstrate a possible application of SACF and GILA, we tested a cr:trRNA against BCL11A (cr:trRNA *BCL11A*, Table 1) that is currently being used in clinical trials (ClinicalTrials.gov: NCT03655678 and

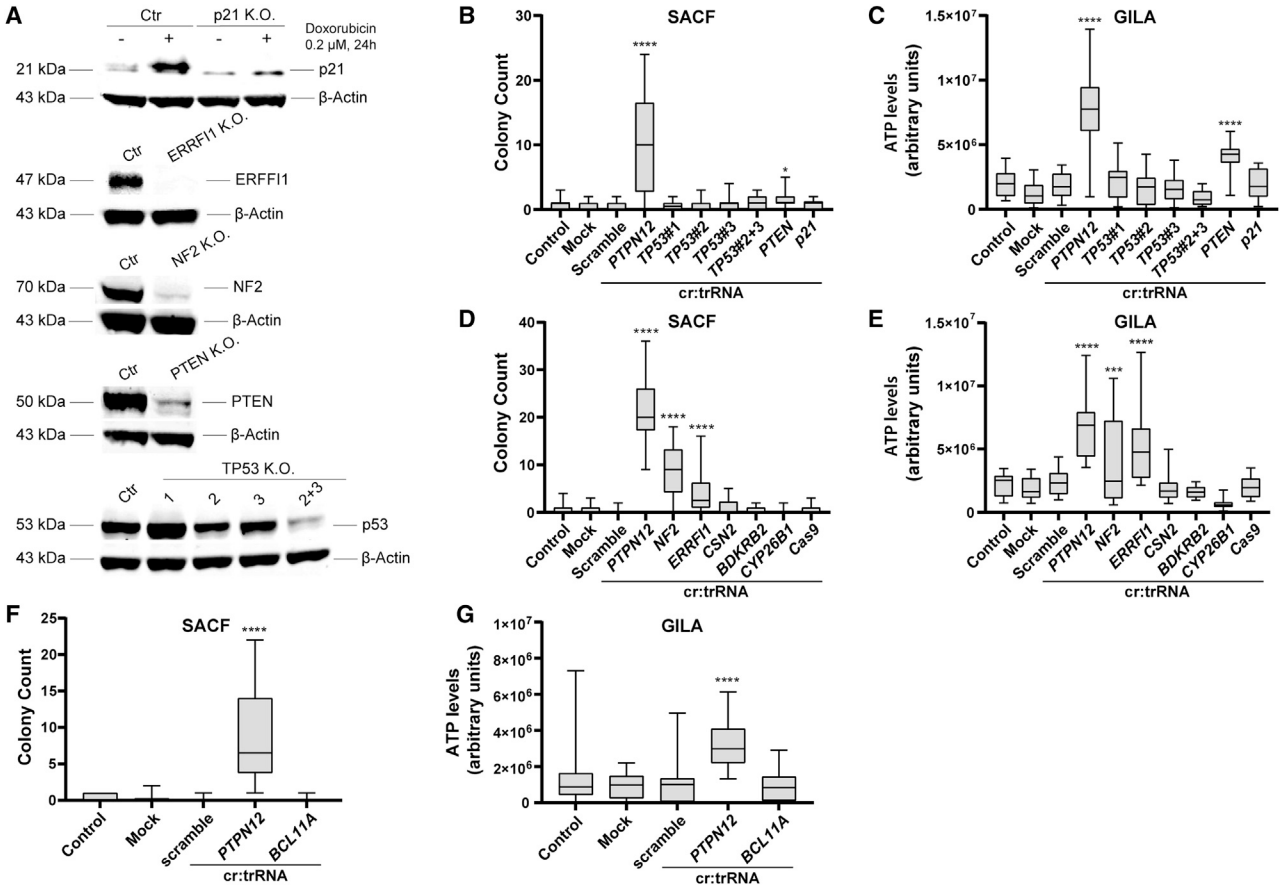


**Figure 3. Identification of positive and negative control genes for *in vitro* transformation**

(A) For each potential positive control, the best cleaving cr:trRNAs from the previously used guide RNA library were selected and tested for protein depletion. 150,000 MCF10A Cas9 cells were electroporated with the cr:trRNA complex and incubated for a week before western blot analysis. Since CDKN1A levels were undetectable in MCF10A Cas9 cells, doxorubicin treatment (0.2 µM, 24 h) was used to induce CDKN1A and confirm its depletion (Ctr = unedited control sample). (B–G) To test the transformation potential of various genes in SACF and GILA, 150,000 cells were electroporated with the corresponding cr:trRNA, and 2,500 cells/well in six replicates were seeded for GILA and SA*CF*. Data of three independent assay repetitions are represented as boxplots. Statistical analysis was performed on the combined data of three assay repetitions using mixed linear regression models for negative binominal (SACF) or Gaussian distribution (GILA) and post hoc Holm-Bonferroni p value adjustment. *p < 0.05, ***p < 0.005, ****p < 0.001 (see Data S1 and S2). See Figure S6 for a representation of the individual assay repetitions.

NCT03745287) for the treatment of β-thalassemia and sickle cell disease (Figures 3F, 3G, S6E, and S6F). These studies evaluate the safety and efficacy of *BCL11A*-edited hematopoietic stem cells. Here, we used MCF10A Cas9 as a surrogate cellular model, since hematopoietic stem cells are suspension cells and hence are inherently able to grow in semisolid medium or spheroids.[54] Both SACF and GILA showed that the selected cr:trRNA *BCL11A* does not induce anchorage independency.

### *In vivo* versus *in vitro* assessment

The conventional method for evaluating the tumorigenic potential of cells is an *in vivo* tumorigenicity study in immune-compromised mice.[10–12] To investigate whether SACF and GILA perform comparably in such *in vivo* tumorigenicity studies regarding the LOD, we injected different ratios (0%, 6%, 12.5%, 25%, 50%, and 100%) of the previously generated pool of stably *PTPN12*-edited cells mixed with parental MCF10A Cas9 cells into NSG mice. The cells were injected either subcutaneously or orthotopically in the mammary fat pad ($10^7$ cells in total), and mice were observed for 22 weeks. In previous experiments, we showed that this cell number and observation time are sufficient to induce tumors when using the breast cancer cell line MDA MB 468 (Figure S9). In this experiment, the injected MCF10A Cas9 cells were not able to form palpable tumors *in vivo* at any PTPN12 edited/unedited cell ratio. Histological analysis of the mammary fat pad confirmed the absence of abnormal growth. Nonetheless, as indicated by the presence of cells positive to the human specific anti-Ku80 antibody (Figure 4), both *PTPN12*-edited and unedited control cells persisted in the mammary fat pad of the orthotopically injected animals. These observations indicate that MCF10A cells, regardless of the PTPN12 status, were able to survive in the murine microenvironment; however, the genetic manipulation of PTPN12 did not induce an obvious measurable growth advantage compared to the parental cell line.

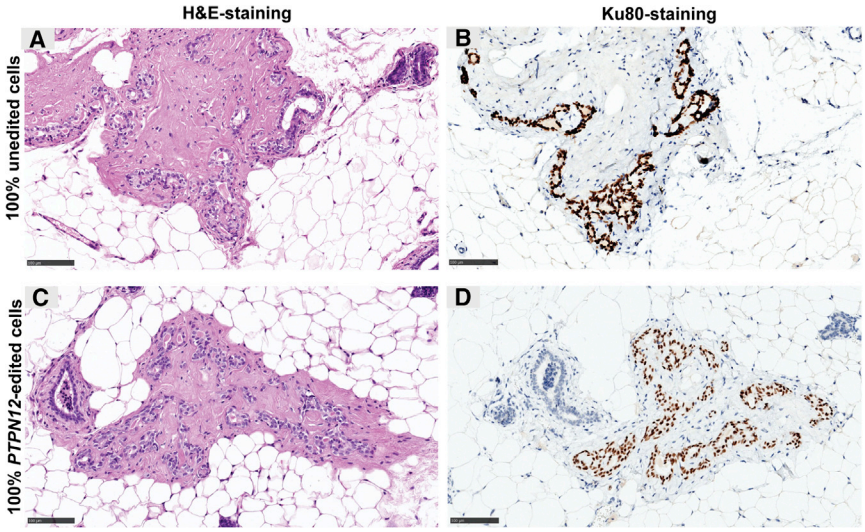


**Figure 4. Persistence of MCF10A Cas9 cells in vivo**

(A–D) *PTPN12*-edited cells were mixed with MCF10A Cas9 parental cells in different ratios (0%, 6%, 12.5%, 25%, 50%, and 100%) and injected in mammary fat pad ($10^7$ cells in total). Mice were sacrificed after 22 weeks and the mammary fat pads were fixed and embedded in paraffin. Histological cross sections were stained with hematoxylin and eosin (A and C) and with an anti-Ku80 antibody (B and D) as a marker for human cells. Ku80-positive cells are shown in brown. Sections of mice injected in the mammary fat pad with 100% control (A and B) or *PTPN12*-edited MCF10A cells (C and D) are represented (scale bars, 100 μm). See also Figure S9.

## DISCUSSION

In this study, we successfully demonstrated that SACF and GILA on MCF10A cells can be used to assess whether human cells acquired the ability to grow anchorage independently upon CRISPR-Cas9 genome editing, and we compared their performance to an *in vivo* tumorigenicity study.

By titrating the amount of cr:trRNA against our positive control *PTPN12*, we showed that SACF has a lower LOD than does GILA, i.e., 6% ± 1% versus 17% ± 4.3%. The better detection limit of SACF was also confirmed when spiking stably PTPN12-edited cells in parental MCF10A Cas9 cells, i.e., 0.8% (SACF) versus 3.1% (GILA). These results indicate a lower detection limit when stably edited cells, rather than freshly electroporated cells, are used. We hypothesize that this is due to technical limits, such as physical cell membrane damage, or due to the accumulation of further mutations during cell expansion/passages.

Since suitable controls are indispensable for the successful validation of any novel assay, we determined a set of CRISPR-Cas9-mediated positive and negative controls. We demonstrated that, in MCF10A Cas9 cells, cr:trRNAs against *CYP26B1*, *BDKRB2*, *CSN2*, and *Cas9* could be used as negative controls, whereas cr:trRNAs against *ERRFI1*, *NF2*, *PTEN*, as well as *PTPN12* could be used as positive controls. We noted that some genes are stronger positive controls in either SACF or GILA. For example, *NF2* was stronger positive in SACF than in GILA, while *PTEN* was strongly positive in GILA and weakly positive in SACF. To detect weakly positive targets, we strongly advise to conduct each assay at least three times and to always perform both SACF and GILA. Of note, the deletion of the tumor suppressor genes *CDKN1A* and *TP53* did not lead to positive results in SACF and GILA. These results are in agreement with previous studies[33,55] demonstrating that the deletion of a tumor suppressor gene might not lead to *in vitro* transformation per se, but potentially to genomic instability and eventually clonal expansion of transformed cells acquiring further mutations.[56–58]

The positive controls identified in MCF10A Cas9 cells were also confirmed in GILA assays with the human immortalized hepatic cell line THLE-2. However, in SACF, the colony count for THLE-2 cells was considerably lower than for MCF10A. These findings suggest that THLE-2 cells could be a suitable cell line for GILA, while more optimization is required to use THLE-2 cells as a surrogate cell line for SA*CF*. The discrepancy in colony-forming efficiency between MCF10A and THLE-2 cells could be due to different reasons, e.g., the longer doubling time of THLE-2 cells (~48 versus ~24 h), which could potentially hinder the expansion of single cells in SA*CF*.

Together with positive and negative controls, we provided an example for the use of SACF and GILA in a preclinical setting by evaluating a therapeutic guide RNA against *BCL11A*.[59] A study by Leibowitz et al.[6] revealed that CRISPR-Cas9 genome editing, among others with the same *BCL11A* guide tested here and in clinical trials, leads to on-target-mediated micronucleus formation and chromothripsis, whose functional consequences are still unclear. Although most chromothripsis occurrences are expected to decrease cell fitness, exceptional cases of transformation could pose a significant safety risk.[6] In this study, we showed that electroporation of MCF10A Cas9 cells with cr:trRNA *BCL11A* did not lead to anchorage-independent growth in SACF as well as GILA. This result could suggest a low transformation risk using *BCL11A* guide RNA in MCF10A cells; however, long-term effects in hematopoietic stem cells still need to be investigated.

PTPN12 impairment is one of the main drivers of triple-negative breast cancer,[49] is involved in early tumorigenesis of hepatocellular carcinoma,[60] and is a marker of poor prognosis in esophageal squamous cell carcinoma and bladder transitional cell carcinoma.[61,62] Thus, PTPN12 loss can be considered as a significant safety risk in genome-edited cells, and its identification in a transformation assay can be deemed valid and provide important information. Interestingly, *PTPN12*-edited MCF10A Cas9 cells were unable to form

tumors in NSG mice, although they led to positive results in GILA and SACF. The absence of tumor growth is consistent with other studies with MCF10A cells reporting that the deletion of ATM (ataxia telangiectasia mutated), a well-known risk factor for breast cancer, or PIK3CA together with TP53 does not give rise to tumors *in vivo*.[63,64] In these cases, the use of *in vitro* assays could provide a more sensitive readout and essential information that may otherwise have been missed. This demonstrates that the inclusion of more sensitive *in vitro* methods such as GILA and SACF in the evolving testing strategy for gene-editing therapeutics is of great importance. In comparison to *in vivo* tumorigenicity studies, which typically last 6–12 months,[20–22] SACF and GILA additionally deliver results in a shorter time frame. Furthermore, SACF and GILA assays are, by far, less costly than tumorigenicity studies in the NSG mouse, enabling more large-scale testing and high-throughput screenings. Moreover, being in concordance with the principles of 3Rs, they also provide a significant animal welfare benefit over current approaches.

A limitation of SACF and GILA is that, by measuring anchorage independency, these assays could only evaluate one of the features of transformation. Related to this, these methods cannot be used on suspension cells, which are anchorage-independent by nature. As the treatment of monogenic blood diseases by gene therapy involves the editing of human hematopoietic stem cells, the development of additional methods based on other properties of transformed cells is strongly needed. For example, a humanized version of the *in vitro* immortalization assay (IVIM), which uses murine hematopoietic stem cells to detect insertional mutagenesis of retroviral vectors,[65,66] would be highly beneficial. Moreover, this study is confined to the MCF10A and THLE-2 cell lines, and the performance in SACF and GILA of other human cell lines, particularly if derived from other tissues, still needs to be investigated. The addition of other cell lines could increase the biological relevance of the *in vitro* transformation assays described herein. Furthermore, validated cell lines could be included in a pre-set panel to predict tumorigenicity in different types of tissues.

Based on our results, we propose a novel test strategy that includes the implementation of SACF and GILA in preclinical safety assessment of gene therapy products, in combination with *in vivo* studies and other known safety assays (Figure S10). SACF and GILA could be used to evaluate candidate crRNAs regarding their safety together with *in silico* (e.g., CALITAS,[67] Cas-OFFinder,[50] CRISPRitz[68]), sequencing, or chromosomal aberration-based methods (e.g., CAST-seq,[69] CIRCLE-seq,[70] DISCOVER-seq,[71] GUIDE-seq,[72] LOOK-seq,[6,73] SITE-seq,[74] karyotyping), and *in vivo* tumorigenicity studies. By screening potential clinical crRNAs in SACF and GILA during the early development phase, unsafe crRNAs could be eliminated early on and valuable resources could be saved. Additionally, in order to reduce the use of animals, SACF and GILA could be conducted prior to an *in vivo* tumorigenicity study, and if clear positive results are obtained, the necessity of a follow-up *in vivo* study could be discussed. SACF and GILA could also be adapted to evaluate the *in vitro* transformation potential of other designer nucleases or viral vectors used for gene therapy. For example, it has been reported that adeno-associated viruses (AAVs) integrate in the human genome in low frequencies, which could lead to insertional mutagenesis and the still debated consequences on tumorigenicity risk.[75,76] In general, adaptation of SACF and GILA for other purposes would require revalidation with suitable controls, e.g., AAV-mediated controls.

In conclusion, our results show that SACF and GILA assays could be valid tools for evaluating the potential transformation risk upon CRISPR-Cas9 genome editing. Once extensive cross-lab validation is successfully accomplished, SACF and GILA could be implemented into a guideline for preclinical safety assessment of gene therapy products, with the aim to reach a global consensus and facilitate the development of such products.

## MATERIALS AND METHODS

### MCF10A Cas9 cell line generation and culture

MCF10A cells were transduced with a lentiviral Cas9 vector as previously described[44–46] and maintained in DMEM/F12 (#11330, Gibco, Thermo Fisher Scientific, Switzerland) supplemented with 5% horse serum (#16050122, Gibco), 20 ng/mL EGF (#PHG0311, Thermo Fisher Scientific), 250 ng/mL hydrocortisone (#H-0888, Sigma, Switzerland), 100 ng/mL cholera toxin (#C8052, Sigma), 10 μg/mL insulin (#1882, Sigma), and 10 μg/mL blasticidin (#15696-096, Gibco) at 37°C under 5% $CO_2$.

### CRISPR-Cas9 genome-wide knockout screen

A CRISPR-Cas9 screen was performed and resulting data were analyzed as previously described.[44–46] A lentiviral library consisting of three pools each containing 66,000 single guide RNAs (sgRNAs) was used to transduce MCF10A Cas9 cells under two conditions (no EGF and 20 ng/mL EGF) with an MOI of 0.5. The sgRNAs against TP53 were present in each pool. For the condition of EGF absence, EGF was removed on day 5 after transduction and the medium was supplied with 0.01% DMSO. Two weeks after infection, DNA was extracted and analyzed by NGS. For data processing, sequencing reads were aligned to the sgRNA library and the individual barcodes of the sgRNAs were quantified. Based on the $\log_2$ fold change of sgRNA levels relative to internal controls, a ranking of gene deletions inducing hyperproliferation was generated for the screen in EGF absence and presence, respectively. The top 100 hits are shown in Table S1. A common ranking was compiled by averaging the ranking of both conditions. The six highest hits were considered for further evaluation. Based on the CRISPR-Cas9 screen, the best performing crRNA sequences (Table S2) for each gene were selected for cleavage efficiency testing, and the best cleaving crRNA was then chosen for SACF and GILA experiments.

### Electroporation of the cr:trRNA complex in MCF10A Cas9 cells

A 40 μM cr:trRNA complex solution was prepared by mixing 100 μM stock solution of crRNA and trRNA with nuclease-free duplex buffer (all IDT, Switzerland) and by heating for 5 min at 95°C. Then, electroporation was performed using the NEON transfection system

(Invitrogen). 150,000 MCF10A Cas9 cells were electroporated with 0.5–12 pmol of the cr:trRNA complex in buffer R at 1,700 V, 20 ms, 1 pulse using 10-μL tips. Afterwards, the cell suspension was transferred to medium and divided into several aliquots for SACF, GILA, and cleavage analysis.

#### Mutation/cleavage efficiency determined by Sanger sequencing and TIDE

DNA was extracted from approximately 100,000 cultured cells 24 h after electroporation using the PureLink genomic DNA kit (#K1820, Thermo Fisher Scientific) according to the manufacturer's instructions. DNA was eluted in 30 μL of elution buffer.

To extract DNA from colonies grown in soft agar, medium was removed and 100 μL of buffer QG (#19063, QIAGEN, Switzerland) was added to dissolve the agar. After a 1-h incubation at 37°C, the solution containing colonies was transferred to microcentrifuge tubes and centrifuged to remove medium and buffer. To extract DNA from low attachment plates, the spheroids were transferred to microcentrifuge tubes and spun down. DNA of cells collected from SACF and GILA was extracted using a NucleoSpin tissue XS kit (#740901, Takara, France) according to the manufacturer's instructions. DNA was eluted in 20 μL of elution buffer.

The region of interest was amplified by PCR using Q5 high-fidelity 2× master mix (#M0492S, New England Biolabs, Switzerland), 1 μM primer (Microsynth, Switzerland), and 10–100 ng of DNA in a 25-μL reaction. The PCR was run with the following steps: 30 s at 98°C, 35 cycles of 5 s at 98°C, 30 s at primer annealing temperature (calculated using a New England Biolabs Tm calculator), 20 s at 72°C, and a final extension step for 5 min at 72°C. Primers (Table S2) were designed approximately 200 bp from the expected cleavage using Primer3 and UCSC *in silico* PCR. The PCR product was purified using the GeneJET PCR purification kit (#K0702, Thermo Fisher Scientific). Primers as well as crRNA sequences for Cas9 deletion were from Kelkar et al.[76] Purified DNA was diluted to 18 ng/100 bp in 12 μL and mixed with 3 μL of forward primer (100 μM) for Sanger sequencing (Microsynth Sanger Sequencing Service). The obtained chromatogram was analyzed using TIDE software[51] with the maximum indel size range.

For visualization of DNA amplicons, DNA was transferred on a 2% agarose gel (#R2081, Thermo Fisher Scientific) in TAE buffer (#786-060, G-Biosciences) and run for 20 min at 180 V.

#### Western blot analysis

Unless otherwise stated, protein lysates were prepared 7 days after electroporation (from approximately $4 \times 10^6$ cells) using 250 μL of radioimmunoprecipitation assay (RIPA) buffer (#89901, Thermo Fisher Scientific), protease inhibitor (#P8340, Sigma, 1:100 dilution), and phosphatase inhibitors (#P044 and #P5726, both 1:100 dilutions). The protein concentration was determined using Pierce Micro BCA (bicinchoninic acid) assay (#23231/#23232/#23234, Thermo Fisher Scientific). 50 μg of each protein lysate was mixed with 4× loading buffer (#NP0007, Thermo Fisher Scientific) and 10× reducing agent (#NP0009, Thermo Fisher Scientific) and heated for 10 min at 70°C before electrophoresis for 65 min at 200 V. Protein transfer to a nitrocellulose membrane was performed using an iBlot dry blotting system (Invitrogen, Thermo Fisher Scientific) according to the manufacturer's instructions. The membrane was blocked from unspecific protein binding for 1 h in blocking buffer (#927-40100, LI-COR Biosciences) before incubating with one of the following primary antibody against PTPN12 (1:5,000 dilution, #ab76942, Abcam, UK), TP53 (1:1,000 dilution, #OP43-L, Sigma), PTEN (1:1,000 dilution, #04-035, Sigma), CDKN1A (1:1,000 dilution, #556431, BD Biosciences, Switzerland), ERRFI1/Mig-6 (1:1,000, #WH0054206M1, Sigma), NF2 (1:1,000 dilution, #12888, Cell Signaling Technology, the Netherlands), and tubulin (1:10,000 dilution, #T6074, Sigma) overnight at 4°C. Secondary antibodies, including IRDye 800CW goat anti-rabbit immunoglobulin G (IgG), IRDye 600CW goat anti-rabbit IgG, IRDye 800CW goat anti-mouse IgG, or IRDye 600CW goat anti-mouse IgG (1:15,000 for IRDye 800 and 1:20,000 for IRDye 600, all LI-COR Biosciences), were incubated for 1 h at room temperature. Proteins were detected using a LI-COR Bioscinces Odyssey infrared-based imager.

#### Generation of a stable *PTPN12*-edited cell pool

The MCF10A Cas9 *PTPN12*-edited cell pool was generated by electroporating 150,000 cells with cr:trRNA PTPN12 #1 (Table S2). Cells were expanded for 4 weeks, mutation frequency was determined by amplicon sequencing (described in Supplemental materials and methods and Figure S4), and protein depletion was verified by western blot. Afterwards, the cells were seeded in SACF and GILA as described below.

#### Soft agar colony-forming assay and statistical analysis

SACF was performed in black 96-well flat and clear-bottom plates with a cell repellent surface (#655976-SIN, Greiner Bio-one, Switzerland). SeaPlaque agarose (#50101, Lonza, Switzerland) was dissolved by heating in water to a final concentration of 1.2% and stored at room temperature until use. To prepare the base layer solution, the solubilized agarose solution was mixed in a 1:1 ratio with filtered 2× DMEM/F12 medium (diluted 10× DMEM/F12, #CAM17-005, GenDEPOT, Katy, TX, USA) containing 20% horse serum, 4 ng/mL EGF, 200 ng/mL cholera toxin, 20 μg/mL insulin, and 1 μg/mL hydrocortisone. 50 μL of base layer solution per well was added to the plate and incubated for 30 min at 4°C. Next, the cell suspension was mixed with the prepared 2× DMEM/F-12 including the mentioned additives and 1.2% agarose solution in a 1:1:1 ratio. 75 μL of cell/well suspension solution (containing 2,500 cells) was added to the plate and immediately solidified at 4°C for 20 min. Afterwards, 100 μL/well MCF10A culture medium was added on top of the soft agar. The plates were incubated for 4 weeks at 37°C under 5% $CO_2$. The medium was changed once a week.

For image analysis, medium was removed and 50 μL/well medium containing 25 nM MitoTracker Red CMXRos (#M7512, Thermo Fisher Scientific) and 1 μg/mL Hoechst 33342 (#62249, Thermo Fisher Scientific) was added. The plate was incubated for 1 h at

37°C before adding 125 μL/well 4.8% (final 2%) formaldehyde (#28908, Thermo Fisher Scientific) solution in PBS and incubating for 30 min at room temperature. Next, the soft agar was washed twice with 100 μL of PBS before adding 75 μL of buffer QG (#19063, QIAGEN) for its solubilization. The plate was incubated for 1 h at 37°C. Afterwards, the plate was imaged and analyzed with the ArrayScan XTI high content analysis reader (Thermo Fisher Scientific) using ×5 magnification in the widefield imaging mode. For each well, 16 images covering the whole well were taken. Analysis of the images was performed with the Thermo Scientific HCS Studio cell analysis software. First, background correction across 100 pixels was applied to the acquired images. Then, signals were smoothed and objects were selected based on size (roughly >1,300 pixels$^2$/3,600 μm$^2$). Additionally, artifacts were excluded based on shape, average intensity, and signal variation of the object. Colonies were primarily selected based on the Hoechst 33342 signal, whereas MitoTracker Red CMXRos was used to exclude contaminant objects.

For statistical analysis, it was anticipated that colony count follows a Poisson distribution, a common model for integer count data.[77] Evaluation of the variance-mean ratio (=dispersion factor)[78] revealed that the SACF data are additionally overdispersed (Data S1). Hence, a negative binominal distribution can be considered appropriate for statistical analysis, as it is also described for the transformed foci count of BALB/c 3T3 cell transformation assays.[79] Significance was thus determined by using a linear regression model for negative binominal distribution with a post hoc Holm-Bonferroni adjustment of p values. To take the three independent assay repetitions of each experiment into account, a mixed effects model was applied with the assay repetition set as a random effect. The sample "Control" was used as reference, and p values <0.05 were considered statistically significant. The R script used for statistical analysis can be found in Data S2, and raw colony count data can be found in Table S3.

#### Growth in low attachment assay and statistical analysis

For GILA, 2,500 cells in 100 μL of medium were seeded in U-bottom, ultra-low attachment plates (#7007, Corning Life Sciences, Switzerland) and incubated for 2 weeks at 37°C under 5% $CO_2$. Before measuring ATP levels, each plate was examined to eliminate from the analysis wells containing contaminant plastic fibers or other objects that enable anchorage-dependent growth. ATP levels were measured using ViaLight Plus cell proliferation and a cytotoxicity bioassay kit (#LT07-221, Lonza) according to the manufacturer's instructions. The luminescent signal was detected using an EnVision 2104 multilabel reader with a 0.5-s measuring time.

For statistical analysis, it was first confirmed that ATP levels follow a Gaussian distribution by generating a quantile-quantile normal plot (Data S1). Then, comparable to SACF data analysis, mixed effect models for Gaussian distribution with a post hoc Holm-Bonferroni adjustment of p values were used to determine significance (Data S2). As described for SACF data, the individual assay repetitions were set as a random effect and the sample control was used as the reference. p values <0.05 were considered statistically significant. Raw ATP data are found in Table S3.

#### *In vivo* tumorigenicity study

Animal experiments were conducted according the Swiss Animal Welfare Law and internal guidelines for the care and use for laboratory animals. The procedures were approved by the Kantonales Veterinäramt Basel-Stadt. NSG mice were purchased from Charles River (France) and acclimatized for 1 week before treatment. Animals were kept in a pathogen-free environment with a controlled 12-h light/12-h dark cycle and *ad libitum* access to a standard rodent diet and water. Cells for injection were trypsinized and prepared in Matrigel (Corning Life Sciences, Switzerland). MCF10A Cas9 *PTPN12*-edited cells were mixed with MCF10A Cas9 cells at different proportions containing 100%, 50%, 12%, or 6% *PTPN12*-edited cells including a 100% wild-type cells control. For each condition, six animals were either injected with $10^7$ cells subcutaneously or in the mammary fad pad. For tumor cell injection, anesthesia was induced in an anesthetic box with 3.5%–4% isoflurane at 0.8–1 L/min of air/$O_2$ (with Oxymat or EverFlo oxygen). Animals were kept under observation for 22 weeks; body weight was measured weekly. For necropsy, mice were euthanized in a $CO_2$ chamber. After euthanasia, the organs and tissues (lung, liver, spleen, lymph nodes, and the injection site [mammary fat pat or skin]) were fixed in 4% neutral buffered formalin, processed, embedded in paraffin wax, and stained with hematoxylin and eosin for histopathology evaluation.

#### Immunohistochemistry analysis

Staining of human cells in mice tissue was performed according to a published protocol, based on the use of a human-specific antibody against Ku80 with proven lack of cross-reactivity against murine tissue.[80] Immunohistochemistry was performed with an anti-Ku80 antibody (#2180, Cell Signaling Technology) and the detection was performed with a biotin-free system using a horseradish peroxidase (HRP)-conjugated UltraMap-anti-rabbit secondary antibody (#052 69717001, Roche Diagnostics, Switzerland) combined with the ChromoMap detection kit (#05266360001, Roche Diagnostics).

#### Data availability statement

All datasets needed to evaluate the conclusions in this study are included in the article and Supplemental information.

## SUPPLEMENTAL INFORMATION

Supplemental information can be found online at https://doi.org/10.1016/j.omtm.2021.09.004.

## ACKNOWLEDGMENTS

We would like to thank L. Bontadelli and Y. Gilbart for technical assistance and T. MacLachlan, T. Schmelzle, K. DiPetrillo, as well as F. Spence for reviewing the manuscript. We also thank L. Villemin and F. von Arx for treating as well as monitoring the mice, and E. Erard for performing staining of the histological tissue sections. Additionally, we would like to thank E. Billy and P. Megel for supporting us in performing the CRISPR-Cas9 screen, and J. Perner

for support on the statistical model. No funding was received in support for this research.

## AUTHOR CONTRIBUTIONS

Conceptualization, M.L., A.d.R.-E., A.O., H.-J.M., and S.L.; methodology, M.L., B.F., M.Z., V.D., A.P., D.M., and S.L.; formal analysis, M.L., A.M., G.K., U.N., and A.P.; investigation, M.L., L.R., U.P.-H., F.S., J.H., V.D., and S.L.; visualization, M.L., U.N., G.K., and V.D.; supervision, A.O., A.d.R.-E., H.-J.M., and S.L.; data curation, G.K. and F.S.; writing – original draft, M.L. and S.L.; writing – review & editing, D.M., L.R., U.P.-H., V.D., A.P., A.d.R.-E., A.O., H.-J.M., and S.L.

## DECLARATION OF INTERESTS

M.L., B.F., M.Z., L.R., G.K., A.d.R.-E., F.S., D.M., V.D., A.P., A.M., U.P.-H., U.N., J.H., H.-J.M., and S.L. were employees of the Novartis Institutes for Biomedical Research at the time this research was conducted. A.O. declares no competing interests.

## REFERENCES


1. Corrigan-Curay, J., O'Reilly, M., Kohn, D.B., Cannon, P.M., Bao, G., Bushman, F.D., Carroll, D., Cathomen, T., Joung, J.K., Roth, D., et al. (2015). Genome editing technologies: defining a path to clinic. Mol. Ther. *23*, 796–806.
2. Hsu, P.D., Scott, D.A., Weinstein, J.A., Ran, F.A., Konermann, S., Agarwala, V., Li, Y., Fine, E.J., Wu, X., Shalem, O., et al. (2013). DNA targeting specificity of RNA-guided Cas9 nucleases. Nat. Biotechnol. *31*, 827–832.
3. Fu, Y., Foden, J.A., Khayter, C., Maeder, M.L., Reyon, D., Joung, J.K., and Sander, J.D. (2013). High-frequency off-target mutagenesis induced by CRISPR-Cas nucleases in human cells. Nat. Biotechnol. *31*, 822–826.
4. Rezza, A., Jacquet, C., Le Pillouer, A., Lafarguette, F., Ruptier, C., Billandon, M., Isnard Petit, P., Trouttet, S., Thiam, K., Fraichard, A., and Chérifi, Y. (2019). Unexpected genomic rearrangements at targeted loci associated with CRISPR/Cas9-mediated knock-in. Sci. Rep. *9*, 3486.
5. Kosicki, M., Tomberg, K., and Bradley, A. (2018). Repair of double-strand breaks induced by CRISPR-Cas9 leads to large deletions and complex rearrangements. Nat. Biotechnol. *36*, 765–771.
6. Leibowitz, M.L., Papathanasiou, S., Doerfler, P.A., Blaine, L.J., Sun, L., Yao, Y., Zhang, C.-Z., Weiss, M.J., and Pellman, D. (2021). Chromothripsis as an on-target consequence of CRISPR-Cas9 genome editing. Nat. Genet. *53*, 895–905.
7. Cullot, G., Boutin, J., Toutain, J., Prat, F., Pennamen, P., Rooryck, C., Teichmann, M., Rousseau, E., Lamrissi-Garcia, I., Guyonnet-Duperat, V., et al. (2019). CRISPR-Cas9 genome editing induces megabase-scale chromosomal truncations. Nat. Commun. *10*, 1136.
8. Ihry, R.J., Worringer, K.A., Salick, M.R., Frias, E., Ho, D., Theriault, K., Kommineni, S., Chen, J., Sondey, M., Ye, C., et al. (2018). p53 inhibits CRISPR-Cas9 engineering in human pluripotent stem cells. Nat. Med. *24*, 939–946.
9. Haapaniemi, E., Botla, S., Persson, J., Schmierer, B., and Taipale, J. (2018). CRISPR-Cas9 genome editing induces a p53-mediated DNA damage response. Nat. Med. *24*, 927–930.
10. World Health Organization (2010). Recommendations for the Evaluation of Animal Cell Cultures as Substrates for the Manufacture of Biological Medicinal Products and for the Characterization of Cell Banks (World Health Organization), https://www.who.int/biologicals/Cell_Substrates_clean_version_18_April.pdf.
11. Sato, Y., Bando, H., Di Piazza, M., Gowing, G., Herberts, C., Jackman, S., Leoni, G., Libertini, S., MacLachlan, T., McBlane, J.W., et al. (2019). Tumorigenicity assessment of cell therapy products: The need for global consensus and points to consider. Cytotherapy *21*, 1095–1111.
12. US Food and Drug Administration (2010). Guidance for industry: Characterization and qualification of cell substrates and other biological materials used in the production of viral vaccines for infectious disease indications, https://www.federalregister.gov/documents/2010/03/04/2010-4553/guidance-for-industry-characterization-and-qualification-of-cell-substrates-and-other-biological.
13. Tappenbeck, N., Schröder, H.M., Niebergall-Roth, E., Hassinger, F., Dehio, U., Dieter, K., Kraft, K., Kerstan, A., Esterlechner, J., Frank, N.Y., et al. (2019). In vivo safety profile and biodistribution of GMP-manufactured human skin-derived ABCB5-positive mesenchymal stromal cells for use in clinical trials. Cytotherapy *21*, 546–560.
14. Silverman, L.I., Dulatova, G., Tandeski, T., Erickson, I.E., Lundell, B., Toplon, D., Wolff, T., Howard, A., Chintalacharuvu, S., and Foley, K.T. (2020). In vitro and in vivo evaluation of discogenic cells, an investigational cell therapy for disc degeneration. Spine J. *20*, 138–149.
15. Fichtner, I., Rolff, J., Soong, R., Hoffmann, J., Hammer, S., Sommer, A., Becker, M., and Merk, J. (2008). Establishment of patient-derived non-small cell lung cancer xenografts as models for the identification of predictive biomarkers. Clin. Cancer Res. *14*, 6456–6468.
16. John, T., Kohler, D., Pintilie, M., Yanagawa, N., Pham, N.-A., Li, M., Panchal, D., Hui, F., Meng, F., Shepherd, F.A., and Tsao, M.S. (2011). The ability to form primary tumor xenografts is predictive of increased risk of disease recurrence in early-stage non-small cell lung cancer. Clin. Cancer Res. *17*, 134–141.
17. Némati, F., Sastre-Garau, X., Laurent, C., Couturier, J., Mariani, P., Desjardins, L., Piperno-Neumann, S., Lantz, O., Asselain, B., Plancher, C., et al. (2010). Establishment and characterization of a panel of human uveal melanoma xenografts derived from primary and/or metastatic tumors. Clin. Cancer Res. *16*, 2352–2362.
18. Bernardo, C., Costa, C., Sousa, N., Amado, F., and Santos, L. (2015). Patient-derived bladder cancer xenografts: A systematic review. Transl. Res. *166*, 324–331.
19. Julien, S., Merino-Trigo, A., Lacroix, L., Pocard, M., Goéré, D., Mariani, P., Landron, S., Bigot, L., Nemati, F., Dartigues, P., et al. (2012). Characterization of a large panel of patient-derived tumor xenografts representing the clinical heterogeneity of human colorectal cancer. Clin. Cancer Res. *18*, 5314–5328.
20. Tentler, J.J., Tan, A.C., Weekes, C.D., Jimeno, A., Leong, S., Pitts, T.M., Arcaroli, J.J., Messersmith, W.A., and Eckhardt, S.G. (2012). Patient-derived tumour xenografts as models for oncology drug development. Nat. Rev. Clin. Oncol. *9*, 338–350.
21. Kawamata, S., Kanemura, H., Sakai, N., Takahashi, M., and Go, M.J. (2015). Design of a tumorigenicity test for induced pluripotent stem cell (iPSC)-derived cell products. J. Clin. Med. *4*, 159–171.
22. Paczulla, A.M., Dirnhofer, S., Konantz, M., Medinger, M., Salih, H.R., Rothfelder, K., Tsakiris, D.A., Passweg, J.R., Lundberg, P., and Lengerke, C. (2017). Long-term observation reveals high-frequency engraftment of human acute myeloid leukemia in immunodeficient mice. Haematologica *102*, 854–864.
23. Kusakawa, S., Yasuda, S., Kuroda, T., Kawamata, S., and Sato, Y. (2015). Ultra-sensitive detection of tumorigenic cellular impurities in human cell-processed therapeutic products by digital analysis of soft agar colony formation. Sci. Rep. *5*, 17892.
24. Vasseur, P., and Lasne, C. (2012). OECD Detailed Review Paper (DRP) number 31 on "Cell Transformation Assays for Detection of Chemical Carcinogens": Main results and conclusions. Mutat. Res. *744*, 8–11.
25. Russell, W.M.S., and Burch, R.L. (1959). The Principles of Humane Experimental Technique (Methuen).
26. Hamburger, A.W., and Salmon, S.E. (1977). Primary bioassay of human tumor stem cells. Science *197*, 461–463.
27. Salmon, S.E., Hamburger, A.W., Soehnlen, B., Durie, B.G.M., Alberts, D.S., and Moon, T.E. (1978). Quantitation of differential sensitivity of human-tumor stem cells to anticancer drugs. N. Engl. J. Med. *298*, 1321–1327.
28. Horibata, S., Vo, T.V., Subramanian, V., Thompson, P.R., and Coonrod, S.A. (2015). Utilization of the soft agar colony formation assay to identify inhibitors of tumorigenicity in breast cancer cells. J. Vis. Exp *20*, e52727.
29. Zhou, Q., and Chai, W. (2016). Suppression of STN1 enhances the cytotoxicity of chemotherapeutic agents in cancer cells by elevating DNA damage. Oncol. Lett. *12*, 800–808.
30. Blumenthal, R.D. (2005). An overview of chemosensitivity testing. Methods Mol. Med *110*, 3–18.
31. Overholtzer, M., Zhang, J., Smolen, G.A., Muir, B., Li, W., Sgroi, D.C., Deng, C.-X., Brugge, J.S., and Haber, D.A. (2006). Transforming properties of YAP, a candidate

oncogene on the chromosome 11q22 amplicon. Proc. Natl. Acad. Sci. USA *103*, 12405–12410.

32. Pires, M.M., Hopkins, B.D., Saal, L.H., and Parsons, R.E. (2013). Alterations of EGFR, p53 and PTEN that mimic changes found in basal-like breast cancer promote transformation of human mammary epithelial cells. Cancer Biol. Ther. *14*, 246–253.

33. Weiss, M.B., Vitolo, M.I., Mohseni, M., Rosen, D.M., Denmeade, S.R., Park, B.H., Weber, D.J., and Bachman, K.E. (2010). Deletion of p53 in human mammary epithelial cells causes chromosomal instability and altered therapeutic response. Oncogene *29*, 4715–4724.

34. Huang, J., Chen, M., Xu, E.S., Luo, L., Ma, Y., Huang, W., Floyd, W., Klann, T.S., Kim, S.Y., Gersbach, C.A., et al. (2019). Genome-wide CRISPR screen to identify genes that suppress transformation in the presence of endogenous *Kras*$^{G12D}$. Sci. Rep. *9*, 17220.

35. Kusakawa, S., Machida, K., Yasuda, S., Takada, N., Kuroda, T., Sawada, R., Okura, H., Tsutsumi, H., Kawamata, S., and Sato, Y. (2015). Characterization of *in vivo* tumorigenicity tests using severe immunodeficient NOD/Shi-scid IL2R$\gamma^{null}$ mice for detection of tumorigenic cellular impurities in human cell-processed therapeutic products. Regen. Ther. *1*, 30–37.

36. Rotem, A., Janzer, A., Izar, B., Ji, Z., Doench, J.G., Garraway, L.A., and Struhl, K. (2015). Alternative to the soft-agar assay that permits high-throughput drug and genetic screens for cellular transformation. Proc. Natl. Acad. Sci. USA *112*, 5708–5713.

37. Sulahian, R., Kwon, J.J., Walsh, K.H., Pailler, E., Bosse, T.L., Thaker, M., Almanza, D., Dempster, J.M., Pan, J., Piccioni, F., et al. (2019). Synthetic lethal interaction of SHOC2 depletion with MEK inhibition in RAS-driven cancers. Cell Rep. *29*, 118–134.e8.

38. Izar, B., Tirosh, I., Stover, E.H., Wakiro, I., Cuoco, M.S., Alter, I., Rodman, C., Leeson, R., Su, M.-J., Shah, P., et al. (2020). A single-cell landscape of high-grade serous ovarian cancer. Nat. Med. *26*, 1271–1279.

39. Mandriota, S.J., Tenan, M., Nicolle, A., Jankowska, J.D., Ferrari, P., Tille, J.-C., Durin, M.-A., Green, C.M., Tabruyn, S., Moralli, D., and Sappino, A.P. (2020). Genomic instability is an early event in aluminium-induced tumorigenesis. Int. J. Mol. Sci. *21*, 9332.

40. Darwiche, R., and Struhl, K. (2020). Pheno-RNA, a method to associate genes with a specific phenotype, identifies genes linked to cellular transformation. Proc. Natl. Acad. Sci. USA *117*, 28925–28929.

41. Pineda, M., Lear, A., Collins, J.P., and Kiani, S. (2019). Safe CRISPR: Challenges and possible solutions. Trends Biotechnol. *37*, 389–401.

42. Ryu, S.-M., Hur, J.W., and Kim, K. (2019). Evolution of CRISPR towards accurate and efficient mammal genome engineering. BMB Rep. *52*, 475–481.

43. You, L., Tong, R., Li, M., Liu, Y., Xue, J., and Lu, Y. (2019). Advancements and obstacles of CRISPR-Cas9 technology in translational research. Mol. Ther. Methods Clin. Dev. *13*, 359–370.

44. Munoz, D.M., Cassiani, P.J., Li, L., Billy, E., Korn, J.M., Jones, M.D., Golji, J., Ruddy, D.A., Yu, K., McAllister, G., et al. (2016). CRISPR screens provide a comprehensive assessment of cancer vulnerabilities but generate false-positive hits for highly amplified genomic regions. Cancer Discov. *6*, 900–913.

45. Liu, H., Golji, J., Brodeur, L.K., Chung, F.S., Chen, J.T., deBeaumont, R.S., Bullock, C.P., Jones, M.D., Kerr, G., Li, L., et al. (2019). Tumor-derived IFN triggers chronic pathway agonism and sensitivity to ADAR loss. Nat. Med. *25*, 95–102.

46. Rago, F., DiMare, M.T., Elliott, G., Ruddy, D.A., Sovath, S., Kerr, G., Bhang, H.C., and Jagani, Z. (2019). Degron mediated BRM/SMARCA2 depletion uncovers novel combination partners for treatment of BRG1/SMARCA4-mutant cancers. Biochem. Biophys. Res. Commun. *508*, 109–116.

47. Hanahan, D., and Weinberg, R.A. (2011). Hallmarks of cancer: The next generation. Cell *144*, 646–674.

48. Soule, H.D., Maloney, T.M., Wolman, S.R., Peterson, W.D., Jr., Brenz, R., McGrath, C.M., Russo, J., Pauley, R.J., Jones, R.F., and Brooks, S.C. (1990). Isolation and characterization of a spontaneously immortalized human breast epithelial cell line, MCF-10. Cancer Res. *50*, 6075–6086.

49. Sun, T., Aceto, N., Meerbrey, K.L., Kessler, J.D., Zhou, C., Migliaccio, I., Nguyen, D.X., Pavlova, N.N., Botero, M., Huang, J., et al. (2011). Activation of multiple proto-oncogenic tyrosine kinases in breast cancer via loss of the PTPN12 phosphatase. Cell *144*, 703–718.

50. Bae, S., Park, J., and Kim, J.-S. (2014). Cas-OFFinder: Afast and versatile algorithm that searches for potential off-target sites of Cas9 RNA-guided endonucleases. Bioinformatics *30*, 1473–1475.

51. Brinkman, E.K., Chen, T., Amendola, M., and van Steensel, B. (2014). Easy quantitative assessment of genome editing by sequence trace decomposition. Nucleic Acids Res. *42*, e168–e168.

52. Kelkar, A., Zhu, Y., Groth, T., Stolfa, G., Stablewski, A.B., Singhi, N., Nemeth, M., and Neelamegham, S. (2020). Doxycycline-dependent self-inactivation of CRISPR-Cas9 to temporally regulate on- and off-target editing. Mol. Ther. *28*, 29–41.

53. Pfeifer, A.M., Cole, K.E., Smoot, D.T., Weston, A., Groopman, J.D., Shields, P.G., Vignaud, J.M., Juillerat, M., Lipsky, M.M., Trump, B.F., et al. (1993). Simian virus 40 large tumor antigen-immortalized normal human liver epithelial cells express hepatocyte characteristics and metabolize chemical carcinogens. Proc. Natl. Acad. Sci. USA *90*, 5123–5127.

54. Zhang, P., Zhang, C., Li, J., Han, J., Liu, X., and Yang, H. (2019). The physical microenvironment of hematopoietic stem cells and its emerging roles in engineering applications. Stem Cell Res. Ther. *10*, 327.

55. Abbas, T., and Dutta, A. (2009). p21 in cancer: Intricate networks and multiple activities. Nat. Rev. Cancer *9*, 400–414.

56. Schedin, P., and Elias, A. (2004). Multistep tumorigenesis and the microenvironment. Breast Cancer Res. *6*, 93–101.

57. Chaffer, C.L., and Weinberg, R.A. (2015). How does multistep tumorigenesis really proceed? Cancer Discov. *5*, 22–24.

58. Wu, X., and Pandolfi, P.P. (2001). Mouse models for multistep tumorigenesis. Trends Cell Biol. *11*, S2–S9.

59. Frangoul, H., Altshuler, D., Cappellini, M.D., Chen, Y.S., Domm, J., Eustace, B.K., Foell, J., de la Fuente, J., Grupp, S., Handgretinger, R., et al. (2021). CRISPR-Cas9 gene editing for sickle cell disease and β-thalassemia. N. Engl. J. Med. *384*, 252–260.

60. Kodama, T., Newberg, J.Y., Kodama, M., Rangel, R., Yoshihara, K., Tien, J.C., Parsons, P.H., Wu, H., Finegold, M.J., Copeland, N.G., and Jenkins, N.A. (2016). Transposon mutagenesis identifies genes and cellular processes driving epithelial-mesenchymal transition in hepatocellular carcinoma. Proc. Natl. Acad. Sci. USA *113*, E3384–E3393.

61. Cao, X., Li, Y., Luo, R.-Z., He, L.-R., Yang, J., Zeng, M.-S., and Wen, Z.-S. (2012). Tyrosine-protein phosphatase nonreceptor type 12 is a novel prognostic biomarker for esophageal squamous cell carcinoma. Ann. Thorac. Surg. *93*, 1674–1680.

62. Piao, Y., Liu, X., Lin, Z., Jin, Z., Jin, X., Yuan, K., and Wu, W. (2015). Decreased expression of protein tyrosine phosphatase non-receptor type 12 is involved in the proliferation and recurrence of bladder transitional cell carcinoma. Oncol. Lett. *10*, 1620–1626.

63. Croessmann, S., Wong, H.Y., Zabransky, D.J., Chu, D., Rosen, D.M., Cidado, J., Cochran, R.L., Dalton, W.B., Erlanger, B., Cravero, K., et al. (2017). *PIK3CA* mutations and *TP53* alterations cooperate to increase cancerous phenotypes and tumor heterogeneity. Breast Cancer Res. Treat. *162*, 451–464.

64. Mandriota, S.J., Buser, R., Lesne, L., Stouder, C., Favaudon, V., Maechler, P., Béna, F., Clément, V., Rüegg, C., Montesano, R., and Sappino, A.P. (2010). Ataxia telangiectasia mutated (ATM) inhibition transforms human mammary gland epithelial cells. J. Biol. Chem. *285*, 13092–13106.

65. Modlich, U., Bohne, J., Schmidt, M., von Kalle, C., Knöss, S., Schambach, A., and Baum, C. (2006). Cell-culture assays reveal the importance of retroviral vector design for insertional genotoxicity. Blood *108*, 2545–2553.

66. Modlich, U., Navarro, S., Zychlinski, D., Maetzig, T., Knoess, S., Brugman, M.H., Schambach, A., Charrier, S., Galy, A., Thrasher, A.J., et al. (2009). Insertional transformation of hematopoietic cells by self-inactivating lentiviral and gammaretroviral vectors. Mol. Ther *17*, 1919–1928.

67. Fennell, T., Zhang, D., Isik, M., Wang, T., Gotta, G., Wilson, C.J., and Marco, E. (2021). CALITAS: A CRISPR-Cas-aware ALigner for *In silico* off-TArget Search. CRISPR J. *4*, 264–274.

68. Cancellieri, S., Canver, M.C., Bombieri, N., Giugno, R., and Pinello, L. (2020). CRISPRitz: Rapid, high-throughput and variant-aware in silico off-target site identification for CRISPR genome editing. Bioinformatics *36*, 2001–2008.

69. Turchiano, G., Andrieux, G., Klermund, J., Blattner, G., Pennucci, V., El Gaz, M., Monaco, G., Poddar, S., Mussolino, C., Cornu, T.I., et al. (2021). Quantitative evaluation of chromosomal rearrangements in gene-edited human stem cells by CAST-seq. Cell Stem Cell *28*, 1136–1147.e5.

70. Tsai, S.Q., Nguyen, N.T., Malagon-Lopez, J., Topkar, V.V., Aryee, M.J., and Joung, J.K. (2017). CIRCLE-seq: A highly sensitive in vitro screen for genome-wide CRISPR-Cas9 nuclease off-targets. Nat. Methods *14*, 607–614.

71. Wienert, B., Wyman, S.K., Yeh, C.D., Conklin, B.R., and Corn, J.E. (2020). CRISPR off-target detection with DISCOVER-seq. Nat. Protoc. *15*, 1775–1799.

72. Tsai, S.Q., Zheng, Z., Nguyen, N.T., Liebers, M., Topkar, V.V., Thapar, V., Wyvekens, N., Khayter, C., Iafrate, A.J., Le, L.P., et al. (2015). GUIDE-seq enables genome-wide profiling of off-target cleavage by CRISPR-Cas nucleases. Nat. Biotechnol. *33*, 187–197.

73. Zhang, C.Z., Spektor, A., Cornils, H., Francis, J.M., Jackson, E.K., Liu, S., Meyerson, M., and Pellman, D. (2015). Chromothripsis from DNA damage in micronuclei. Nature *522*, 179–184.

74. Cameron, P., Fuller, C.K., Donohoue, P.D., Jones, B.N., Thompson, M.S., Carter, M.M., Gradia, S., Vidal, B., Garner, E., Slorach, E.M., et al. (2017). Mapping the genomic landscape of CRISPR-Cas9 cleavage. Nat. Methods *14*, 600–606.

75. Deyle, D.R., and Russell, D.W. (2009). Adeno-associated virus vector integration. Curr. Opin. Mol. Ther. *11*, 442–447.

76. McCarty, D.M., Young, S.M., Jr., and Samulski, R.J. (2004). Integration of adeno-associated virus (AAV) and recombinant AAV vectors. Annu. Rev. Genet. *38*, 819–845.

77. Coxe, S., West, S.G., and Aiken, L.S. (2009). The analysis of count data: A gentle introduction to poisson regression and its alternatives. J. Pers. Assess. *91*, 121–136.

78. Cameron, A.C., and Trivedi, P.K. (1990). Regression-based tests for overdispersion in the Poisson model. J. Econom. *46*, 347–364.

79. Hoffmann, S., Hothorn, L.A., Edler, L., Kleensang, A., Suzuki, M., Phrakonkham, P., and Gerhard, D. (2012). Two new approaches to improve the analysis of BALB/c 3T3 cell transformation assay data. Mutat. Res. *744*, 36–41.

80. Allard, J., Li, K., Lopez, X.M., Blanchard, S., Barbot, P., Rorive, S., Decaestecker, C., Pochet, R., Bohl, D., Lepore, A.C., et al. (2014). Immunohistochemical toolkit for tracking and quantifying xenotransplanted human stem cells. Regen. Med. *9*, 437–452.